Flight Control Oriented Bottom-up Nonlinear Modeling of Aeroelastic Vehicles

Béla Takarics, Bálint Vanek
Systems and Control Lab
Institute for Computer Science and Control
Hungarian Academy of Sciences
Kende u. 13-17.
1111 Budapest, Hungary
+36 1 279 6000
{takarics.bela, vanek.balint}@sztaki.mta.hu

Aditya Kotikalpudi
Systems Technology Inc.
Hawthorne, CA 90250
aditya@systemstech.com

Peter Seiler
University of Minnesota
Minneapolis, MN 55455
seile017@umn.edu

Abstract—The fuel efficiency of future aircraft can be improved by reducing the weight and structure and by increasing the wingspan. This makes the aircraft structure more flexible and results in increased aeroservoelastic (ASE) effects. The use of active control systems to suppress ASE effects is an important aspect for future flight control systems. The basis of active control system design is an appropriate control oriented model, usually given in the linear parameter-varying (LPV) framework. The ASE model is based on the integration of aerodynamics, structural dynamics and flight dynamics. These subsystems can be developed separately and combined to form the ASE model. The dynamic order of such ASE models is usually too large for control synthesis and implementation. Thus, model order reduction is required. However, model order reduction of LPV systems can still lead to challenges. The aim of the paper is to overcome this reduction step by using a "bottom-up" modeling approach. The main idea is to use low order, simple subsystems and/or reduce them before integrating them into the nonlinear model. Therefore, a low order control oriented model is created that captures the key ASE dynamics of the aircraft. An important benefit of this modeling approach is that the physical meaning of the states is retained. The specific flexible aircraft example is the mini MUTT (Multi Utility Technology Testbed) vehicle. The bottom-up modeling approach, by reducing the linear structural dynamics and the parameter dependent aerodynamics subsystems, resulted in a 33 state low order nonlinear model (LOM). The nonlinear model is then linearized about a family of "trim points" by Jacobian linearization leading to a grid based LPV model. A full order model (FOM) is developed in order to evaluate the accuracy of the 33 state LOM. The FOM is developed in the same way as the LOM. However, the subsystems are not reduced in this case, leading to a 97 states model. The accuracy of the low order model is confirmed by evaluating the ν-gap metric with respect to the full order model and by time domain simulations.

TABLE OF CONTENTS

1. INTRODUCTION

The fuel efficiency of future aircraft can be improved by reducing the weight and structure and by increasing the wingspan. This makes the aircraft structure more flexible and increases aeroservoelastic (ASE) effects. Aeroelastic flutter involves the adverse interaction of aerodynamics with structural dynamics and produces an unstable oscillation [1]. The use of active control systems to suppress ASE effects is an important aspect for future flight control systems. Active control system design is based on an appropriate control oriented model [2–6]. A natural approach to model ASE systems for control design is the linear parameter-varying (LPV) [7,8] framework, which captures the parameter varying dynamics of the aircraft. The paper focuses on the grid-based LPV framework [9]. A grid based LPV model can be obtained by linearizing the nonlinear model over a set of equilibrium points [10].

Modeling ASE systems is based on the integration of aerodynamics, structural dynamics and flight dynamics [11–15]. These models are developed separately and combined to form the ASE model. Depending on the modeling approach and the assumptions/approximations involved, the resulting ASE models can be highly coupled nonlinear equations. The paper focuses on ASE models with the following assumptions. The unsteady aerodynamics is modeled using the doublet lattice method (DLM) [16]. The structural dynamics model is obtained from a finite element model (FEM) by linear Euler beams. The nonlinear equations of motions are derived based on a mean axes reference frame [17–19]. The mean axes approach describes the dynamics of the flexible body by a set of equations which decouple the rigid body modes from the vibrational modes. The mean axes coordinates ensure that the coupling is restricted to external forcing terms only [19]. The mean axes are a floating reference frame in which the dynamics of the flexible aircraft can be defined. The axes move with respect to an inertial frame as the elastic body moves but they are not attached to any material point on the body itself. The translation and rotation of the axes are governed by a specific set of equations known as the mean axes constraints. The resulting ASE model is a set of equations of motion that is an extension of the well known rigid body equations. The limitations of the approach are given in [20]. Response to [20] is given in [21]. Additional research was carried out by [13, 18, 22] to resolve the unclear aspects of the mean axes derivations.

The structural dynamics and DLM based aerodynamics make the dynamic order of the ASE models too large for control synthesis and implementation. Thus, model order reduction is required before the control synthesis step. This is in general done in the following way. First, a grid based LPV

model is obtained from the nonlinear ASE model. Second, the resulting LPV model is reduced by LPV model order reduction techniques. However, model order reduction of LPV systems is still not a completely straightforward task. Recent LPV model order reduction approaches can be found in [23–28]. The aim of the paper is to overcome the LPV reduction step by a "bottom-up" modeling approach. The key idea is the following. The FEM and DLM based subsystems modeling the structural dynamics and the aerodynamics have simpler structure than the combined ASE model. Thus, the order of these subsystems can be reduced by the application of simpler, more tractable reduction techniques. The key considerations for building low order subsystems are the following. The actuator bandwidth for ASE aircraft determines the modes that can be effectively controlled. Thus, the linear structural model needs to include only the lower frequency modes that lie within the actuator bandwidth. The DLM based unsteady aerodynamic model has a continuous state space form with special properties. This can be efficiently reduced, for example as given in [29]. Combining these reduced order subsystems results in a low order nonlinear ASE model. A grid based LPV model can then be obtained by Jacobian linearization. The resulting LPV model is suitable for control synthesis. On the one hand, it is of sufficiently low order. On the other hand, it is capable of capturing the key aeroelastic behavior of the flexible aircraft. An important benefit of such "bottom-up" modeling approach is that the physical meaning of the states is preserved. Therefore, the interpolation between the LPV grid points can be easily solved.

The resulting LPV model can be further reduced if necessary, for example by LPV balanced reduction [23] that is limited to systems with low dynamic order [24, 25].

The specific flexible aircraft example is the mini MUTT (Multi Utility Technology Testbed) [30] vehicle described in Section 2. The aircraft and the software for the FEM model and DLM aerodynamics are built at the University of Minnesota [12, 31]. The "bottom-up" modeling based nonlinear ASE model is derived in Section 2. A grid based LPV model is obtained in Section 3. The accuracy of the low order LPV model is assessed in Section 4, which is followed by the Conclusions.

2. AEROSERVOELASTIC MODEL

The current section describes the main considerations and assumptions leading to the development of the nonlinear ASE model. The aircraft under consideration is the mini MUTT aircraft [30]. The mini MUTT is based on the aerodynamic design of the Body Freedom Flutter (BFF) vehicle built by Lockheed Martin and the Air Force Research Laboratory [32]. The aircraft exhibits the so called body freedom flutter, in which the first wing bending mode couples with the rigid short period mode to create instability which can lead to loss of aircraft [2]. Figure 1 depicts the mini MUTT aircraft.

The aircraft has 8 control surfaces, 4 on each side. These are termed $L1$, $L2$, $L3$, $L4$, $R1$, $R2$, $R3$ and $R4$, where $L1$ and $R1$ are located on the body and $L4$ and $R4$ are located at the wing tips. Control surfaces $L2$ and $R2$ are used as ailerons and $L3$ and $R3$ as elevators while the remaining control surfaces are used for flutter suppression. A Futaba S9254 servo is used as actuator on the mini MUTT. A second-
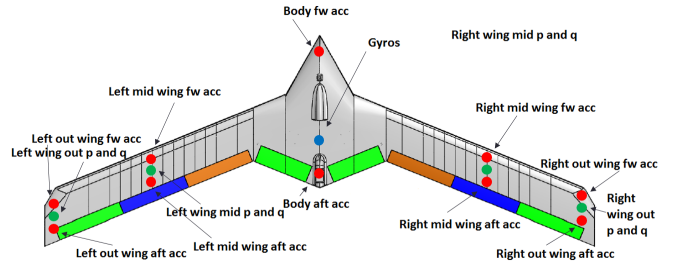

Figure 1: mini MUTT aircraft

order model

$$G_{act}(s) = \frac{96710}{s^2 + 840s + 96710} \qquad (1)$$

is constructed via frequency-domain identification techniques using a chirp input signal. Validation is performed in the frequency domain using a second set of data with an input chirp at a higher voltage and in the time domain via step response data [33]. The Futaba S9254 servo has a bandwidth of approximately 133 rad/s. Therefore, the frequency region of interest of the ASE model is chosen to be up to 100 rad/s.

The aircraft has 30 sensors in total. 12 of these sensors are located at the center of gravity (CG) of the undeformed body. These measured outputs are the attitude angles ϕ and θ, angular rates p, q and r, accelerations a_x, a_y and a_z, absolute value of the ground speed without wind components V_s, angle of attack α, sideslip angle β and flight path angle γ. There are 18 additional accelerometers and angular rate sensors located on the body, at the middle of the wing or at the wing tips to measure the effects of elastic deformation. The sensors with their positions are given in Figure 1. The coordinate systems of the sensors located on the wing are aligned with the sweep angle of the wing.

The ASE model is based on a subsystem approach as shown in Figure 2. The modeling of the subsystems is discussed further in the following subsections.
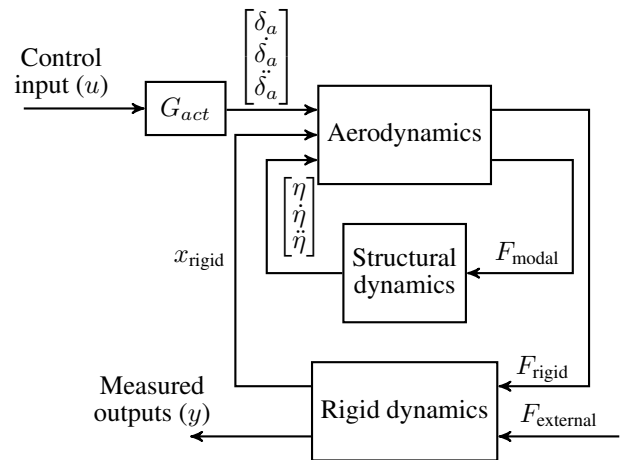

Figure 2: ASE subsystem interconnection

Rigid Body Dynamics - Mean Axes Constraints

The following section reviews the key points of the mean axes based derivation of the equations of motion for flexible

2

aircraft. The reference frame of the aircraft is chosen such that it satisfies the translational and rotational mean axes constraints. The translational mean axes constraint states that there is no net generation of internal translational momentum [17, 19]. The nonlinear rotational mean axes constraint states that there is no net generation of internal angular momentum [13, 17, 18]. The mean axes reference frame always exists [17]. However, in general it is non trivial to identify. Therefore, the practical mean axes can be introduced. The practical mean axes satisfies an approximate angular momentum condition, the so called linear rotational constraint [19].

The following assumptions are were made for the derivation of the nonlinear equations of the ASE model.

Assumption 1: The instantaneous inertia tensor is equivalent to the undeformed, or rigid body, inertia tensor J_{rig}.

Assumption 2: All derivatives of the inertia tensor are assumed to be zero.

It was shown in [18, 22] that in case of straight and level flight or flight with only gentle maneuvers the coupling terms resulting from the rotation rate will be very small.

Assumption 3: It is assumed that the elastic deformation occurs primarily in one direction within the reference frame, meaning that the deflection and deflection rates are collinear. If collinear, the deflection and deflection rates satisfy

$$\delta_i \times \frac{d}{dt}\bigg|_{\text{rel}} \delta_i = 0 \qquad (2)$$

where δ_i stands for the elastic deformation of the ith particle of the deformable body.

The nonlinear rotational constraint and the linear rotational constraint are equivalent based on Assumption 3. The assumption of collinearity is typically valid for beam and plate-like structures [14, 34].

Under Assumptions 1 and 2 the nonlinear equations of motions simplify as

$$\begin{bmatrix} mI & 0 \\ 0 & J_{\text{rig}} \end{bmatrix} \begin{bmatrix} \dot{V}_{\text{r}} \\ \dot{\Omega}_{\text{r}} \end{bmatrix} + \begin{bmatrix} mI\Omega_{\text{r}} \times V_{\text{r}} \\ \Omega_{\text{r}} \times J_{\text{rig}}\Omega_{\text{r}} \end{bmatrix} = \begin{bmatrix} \sum F_i \\ \sum M_i \end{bmatrix} \qquad (3)$$

where m and J_{rig} are the mass and rigid inertia of the aircraft, V_{r} and Ω_{r} the translational and angular velocities in the mean axes with respect to inertial axes and F_i and M_i are the forces and moments along the mean axes.

Further details about Newtonian and Lagrangian based derivations of the equations of motions for flexible aircraft in the mean axes framework can be found in [18] and [19] respectively.

FEM Structural Dynamics

The structural model of the mini MUTT aircraft is developed based on a Finite Element (FE) approach [12, 13]. A common element in such applications is the Euler-Bernoulli-beam with added torsional effects. The interconnection of the beams is shown if Figure 3.

The mass distribution of the wing is assumed to be replaced by a concentrated mass system based on physical considerations of components such as winglets, actuators, flight
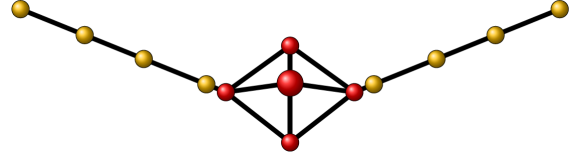
Figure 3: FEM model of the mini MUTT aircraft [13]

computer and other electronics. The center body of the aircraft is assumed rigid. Therefore, the beams corresponding to the center body have very high stiffness. The model has 14 nodes interconnected with beams which have 3 degrees of freedom - heave, twist and bending. The resulting FEM model has 12 modes and the development details are given in [11, 12, 31].

The structural model can be written as

$$\mathcal{M}\ddot{\eta} + \mathcal{C}\dot{\eta} + \mathcal{K}\eta = \mathcal{F} \qquad (4)$$

where $\mathcal{M}$, $\mathcal{C}$ and $\mathcal{K}$ are the modal mass, damping and stiffness matrices respectively, η is the modal coordinate vector and $\mathcal{F}$ is the external excitation in modal coordinates.

The elastic deformation of the nodes can be written as a summation of the elastic mode shapes Φ_i multiplied by their respective modal coordinates η_i.

$$\delta = \begin{bmatrix} \delta_1 \\ \vdots \\ \delta_n \end{bmatrix} = \sum_j \Phi_j \eta_j = \Phi\eta \qquad (5)$$

Modal mass orthogonality is assumed which leads to the following conditions for the vibration modes of unrestrained bodies [18, 19, 34, 35].

$$\sum_i m_i \delta_i = 0 \qquad (6)$$

$$\sum_i m_i \frac{d}{dt}\bigg|_{\text{rel}} \delta_i = 0 \qquad (7)$$

$$\sum_i m_i \boldsymbol{s}_i \times \frac{d}{dt}\bigg|_{\text{rel}} \delta_i = 0 \qquad (8)$$

where m_i is the mass of the ith particle, s_i denotes the undeformed position of the ith particle in the inertial frame. Equation (6) states that the vibration modes do not displace the center of mass. Equation (7) states that the vibration modes do not generate any net translational momentum, which is identical to the translational mean-axis condition. Equation (8) states that the vibration modes do not generate any net approximate angular momentum, which is identical to the linear rotational mean-axis constraint [18].

The structural dynamics model is reduced in the following way. As pointed out before, the actuator bandwidth sets a limit for the frequency region of interest. Therefore, only the first 4 modes fall in the frequency region of interest. The remaining 8 modes are truncated from the linear structural dynamics model. The resulting structural dynamics model has 8 states, $\eta_{1\dots4}$ and $\dot{\eta}_{1\dots4}$.

Aerodynamics

Doulbet Lattice Method aerodynamics—The aerodynamics for the mini MUTT aircraft is modeled with the subsonic

DLM [16, 31] along with a standard vortex lattice method (VLM) to take care of the steady part [36]. The model is divided into aerodynamic panels as shown in Figure 4.
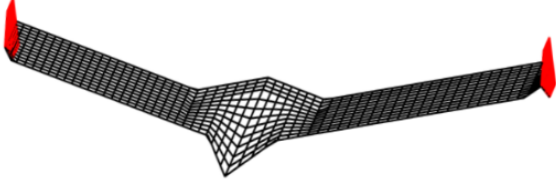
Figure 4: Aerodynamic grid of the mini MUTT aircraft [31]

The following aerodynamic derivation is a short summary based on [13, 31]. The DLM results in the AIC (Aerodynamic Influence Coefficient) matrices that relate the normalwash vector $\bar{w}$ to the normalized pressure difference vector $\bar{p}$ about the panels as

$$\bar{p} = [AIC(\omega, V)]\,\bar{w} \qquad (9)$$

where ω is the oscillating frequency and V is the air speed. These two parameters are in general transformed into a single dimensionless parameter, the reduced frequency

$$k = \frac{\omega \bar{c}}{2V} \qquad (10)$$

where $\bar{c}$ is the reference chord length of the aircraft. The resulting aerodynamic force F_{aero} can be calculated as

$$F_{aero} = \bar{q} S_p\,[AIC(k)]\,\bar{w} \qquad (11)$$

where $\bar{q}$ is the free stream dynamic pressure and S_p is the panel area matrix. The aerodynamic model is connected with the structural dynamic model in two steps. First, the nodal displacements δ_i are projected on the aerodynamic model resulting in the normalwash vector $\bar{w}$. Second, the aerodynamic force F_{aero} is transformed to modal coordinates F_{modal}. The connection is done by splining interpolation. The normalwash vector can be calculated from the modal displacement vector as

$$\bar{w} = (D_1 + ikD_2)\,T_{as}\Phi\eta \qquad (12)$$

where D_1 and D_2 are the differentiation matrices and T_{as} is the interpolation matrix that projects the structural grid deformation on to the aerodynamic panels in form of their pitch and heave deformation [37]. The aerodynamic force distribution can now be written as

$$F_{aero} = \bar{q} S\,[AIC(k)]\,(D_1 + ikD_2)\,T_{as}\Phi\eta \qquad (13)$$

where S is the integration matrix. The force distribution in modal coordinates can be obtained as

$$F_{modal} = \Phi^T T_{as}^T F_{aero} \qquad (14)$$

Combining (13) and (14) and leaving out the dynamic pressure and modal coordinate results in the so called generalized aerodynamic matrix (GAM)

$$Q(k) = \Phi^T T_{as}^T S\,[AIC(k)]\,(D_1 + ikD_2)\,T_{as}\Phi \qquad (15)$$

The GAM maps the modal deformation η to the aerodynamic force distribution in modal coordinates F_{modal} as

$$F_{modal} = \bar{q}\,[Q(k)]\,\eta \qquad (16)$$

Since the GAM matrices are frequency dependent the resulting aerodynamic model is dynamic. It is important to emphasis that the GAM matrices are obtained only over a discrete reduced frequency grid. However, time domain aeroelastic simulations require a continuous model. There are several methods to obtain such models. Roger's rational function approximation (RFA) method [38] is applied. The resulting aerodynamic model is obtained in the form

$$Q_{panel}(k) = Q_{panel_0} + Q_{panel_1}ik + Q_{panel_2}(ik)^2 +$$
$$\sum_{l=1}^{n_p} Q_{panel_{l+2}} \frac{ik}{ik + b_l} \qquad (17)$$

where Q_{panel_0}, Q_{panel_1} and Q_{panel_2} stand for the quasi-steady, velocity and acceleration terms of the aerodynamic model. The $Q_{panel_{l+2}}$ terms take the lag behavior of the aerodynamic model into account. The poles of the lag states are given by b_l. n_p number of poles are selected for each modal coordinate a priori. This implies that the resulting aerodynamic model in general is of much higher dimension than the structural model.

The aero lag terms can be given in the following state space form

$$\dot{x}_{aero} = \frac{2V}{\bar{c}} A_{lag} x_{aero} + B_{lag} \begin{bmatrix} \dot{x}_{rigid} & \dot{\eta} & \dot{u} \end{bmatrix}^T \,||$$
$$y_{aero} = C_{lag} x_{aero} \qquad (18)$$

Such form of the GAM matrix results in a linear parameter-varying (LPV) aerodynamic model that is affine with the square of the airspeed. The number of lag states and structural modes taken into account to develop the aeroelastic model influences how accurate the aerodynamic and structural models are respectively. The resulting number of the aerodynamic states can be given as

$$n_{x_{aero}} = n_{lag_{poles}} \times (n_{rigid} + n_\eta + n_{input}) \qquad (19)$$

Note that RFA form of the GAM matrix given as (17) requires the rigid states, the modal coordinates η, input u and their the first and second time derivatives as input parameters.

A low order DLM model is derived in the following way. First, the GAM matrices are obtained based on the reduced set of 4 elastic modes leading to 36 lag states. Note that in [31] 12 elastic modes are used, leading to a 52 state aerodynamic model. Second, a minimal realization for the state space model defined by A_{lag}, B_{lag} and C_{lag} is applied. This step removes 22 states, resulting in a 14 state unsteady aerodynamics. Third, a linear balancing transformation matrix T is computed for the 14 state aerodynamic model given by $A_{lag_{14}}$, $B_{lag_{14}}$ and $C_{lag_{14}}$. A 4 state aerodynamic model is obtained by residualizing the 10 states with the smallest Hankel singular values. Note that other methods, for example [29], can be also applied to obtain a low order aerodynamic model.

Rigid body aerodynamics and throttle model—Since the structural grid points have 3 degrees of freedom, the VLM/DLM based aerodynamic model described in the previous section provides lift force, roll and pitch moments. The drag and side forces with yaw moment are modeled via classical aerodynamic models. These models are based on the rigid version of the mini MUTT aircraft. The throttle model has 1 state and provides propulsion forces and moments. The rigid body aerodynamic coefficients and the throttle model is available at the UAV group of the University of Minnesota http://www.uav.aem.umn.edu/.

4

Output Equations

Equation (3) results in the accelerations and angular rates in the mean axes. In case of flexible vehicles the sensor measures the total local accelerations or angular rates, which would include the effects of the elastic deformations [19]. Consequently, the local angular rates can be given as

$$\Omega_{\text{local}} = \Omega_{\text{r}} + \Phi_{\text{ang}}\dot{\eta} \qquad (20)$$

where Φ_{ang} contains the mode shapes for angular elastic deformation. The local accelerations are similarly affected by the elastic deformation. The local accelerations can be given as

$$a_{\text{local}} = a_{\text{r}} + \Phi_{\text{trans}}\ddot{\eta} \qquad (21)$$

where Φ_{trans} contains the mode shapes for translational elastic deformation. The rigid body acceleration vector a_{r} at the sensor location p is given by

$$a_{\text{r}} = \frac{d}{dt}\bigg|_{\text{rel}} V_{\text{r}} + \Omega_{\text{local}} \times V_{\text{r}} + \Omega_{\text{local}} \times \Omega_{\text{local}} \times p + \frac{d}{dt}\bigg|_{\text{rel}} \Omega_{\text{local}} \times p \qquad (22)$$

For simplicity, it is assumed that the accelerometers and rate sensors of the mini MUTT aircraft are aligned with the structural model grid nodes.

The Resulting Nonlinear ASE Model

Combining the components described above leads to the nonlinear ASE model of the mini MUTT aircraft. The model has 33 states. These include 8 rigid body states (attitude angles ϕ and θ, angular rates p, q and r and velocity u, v and w); 8 structural dynamics states (modes $\eta_{1\ldots4}$ and $\dot{\eta}_{1\ldots4}$); 4 aerodynamics states $x_{aero_{1\ldots4}}$; 12 actuator states of the 6 servos (2 state servos for the aileron, elevator and $L1$, $L4$, $R1$ and $R4$ flaps); 1 state of the throttle model.

3. LPV MODEL OF THE MINI MUTT AIRCRAFT

The aim of this section is to derive an LPV model of the mini MUTT aircraft. An LPV system is described by the state space model

$$\dot{x}(t) = A(\rho(t))\,x(t) + B(\rho(t))\,u(t) \qquad (23a)$$
$$y(t) = C(\rho(t))\,x(t) + D(\rho(t))\,u(t) \qquad (23b)$$

with the continuous matrix functions $A\colon \mathcal{P} \to \mathbb{R}^{\times}$, $B\colon \mathcal{P} \to \mathbb{R}^{\times}$, $C\colon \mathcal{P} \to \mathbb{R}^{\times}$, $D\colon \mathcal{P} \to \mathbb{R}^{\times}$, the state $x\colon \mathbb{R} \to \mathbb{R}$, input $u\colon \mathbb{R} \to \mathbb{R}$, output $y\colon \mathbb{R} \to \mathbb{R}$ and a time-varying scheduling signal $\rho\colon \mathbb{R} \to \mathcal{P}$, where $\mathcal{P}$ is a compact subset of $\mathbb{R}^{\rho}$. The parameter vector ρ may include elements of the state vector x, in this case the system belongs to the class of quasi LPV models. In a grid representation, the LPV system is described as a collection of LTI models $(A_k, B_k, C_k, D_k) = (A(\rho_k), B(\rho_k), C(\rho_k), D(\rho_k))$ obtained from evaluating the LPV model at a finite number of parameter values $\{\rho_k\}_1^{n_{\text{grid}}} = \mathcal{P}_{\text{grid}} \subset \mathcal{P}$.

The grid based LPV model of the mini MUTT aircraft can be obtained from the nonlinear ASE model by Jacobian linearization as given in [10]. The aircraft is first trimmed for straight and level flights at various airspeeds after which the linearization is carried out. Therefore, the scheduling parameter is defined as $\rho = V_s$ in the interval $[16, 30]\ m/s$ over a grid of 141 equidistant points. Note that since ρ

depends on rigid body states u, v and w, the developed model of the mini MUTT aircraft belongs to the class of quasi LPV systems. The pole migration of the LPV model is given in Figure 5. Flutter occurs at $23.5\ m/s$ airspeed at $25.6\ rad/s$. Based on the pole migrations it can be also concluded that the aircraft has unstable spiral mode at low speed which goes stable at higher speeds.
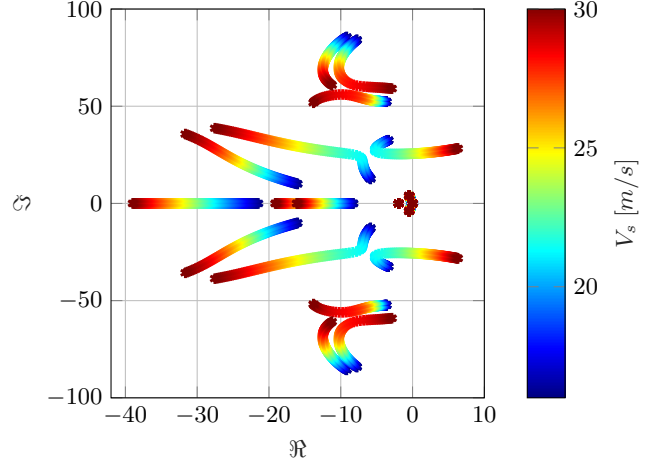

**Figure 5**: Pole migration of the 33 state mini MUTT aircraft

4. ASSESSMENT OF THE LPV MODEL

The objective of the proposed bottom-up modeling approach is to obtain low order models suitable for the design of an active aeroservoelastic control law that also performs well on a higher fidelity system. A high fidelity nonlinear ASE model, termed full order model (FOM), is developed based on the same assumptions and subsystem modeling approach as in case of the 33 state low order model. The only difference is that the subsystems are not reduced before combining them into the ASE model. Specifically, the original 12 modal coordinates of the structural dynamics are retained and the unsteady aerodynamic model also retains the original 52 states. Therefore, the full order ASE nonlinear model has 97 states. In addition, an LPV model of the full order model is derived in the same way as for the 33 state model.

Comparison with the Full Oder LPV model

The "bottom-up" modeling based 33 state LPV model is compared with the 97 state full order LPV model based on several aspects.

Pole migration—Figure 6 shows the pole migrations of the low and full order LPV models. The high frequency poles of the full order model are not shown in the figure for better visibility. The poles of both models migrate on a very similar trajectory. The full order LPV model predicts flutter at 24 m/s with 26.1 rad/s frequency and the low oder model has 23.5 m/s flutter speed with 25.6 rad/s. The flutter speed and frequency accuracy of the low order model is good enough for control design.
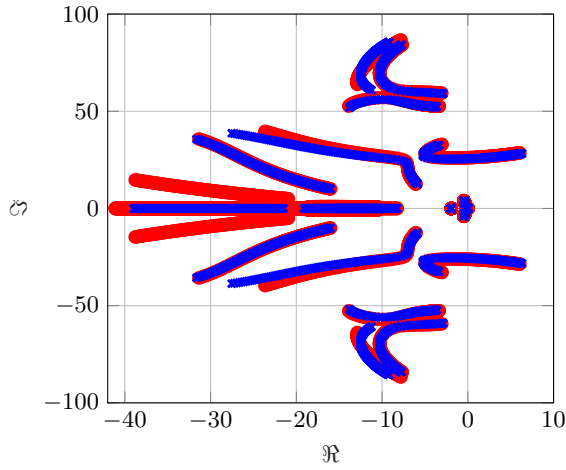
Figure 6: Pole migrations the 33 (——×——) and 97 (——o——) states LPV models

ν-gap metric—The $ν$-gap metric $δ_ν(\cdot, \cdot)$ is used as a measure since it takes into account the feedback control objective. It takes values between zero and one, where zero is attained for two identical systems. A system P_1 that is within a distance $ε$ to another system P_2 in the $ν$-gap metric, i.e. $δ_ν(P_1, P_2) < ε$, will be stabilized by any feedback controller that stabilizes P_2 with a stability margin of at least $ε$. [39] A plant at a distance greater than $ε$ from the P_2, on the other hand, will in general not be stabilized by the same controller. The $ν$-gap metric thus captures the likelihood that a feedback controller designed on the low order model will perform well on the full order model. It can be calculated frequency by frequency as

$$
\begin{aligned}
δ_ν(P_1(\mathrm{j}\,ω)\,, P_2(\mathrm{j}\,ω)) = \\
\| \left(I + P_2(\mathrm{j}\,ω)\ P_2^*(\mathrm{j}\,ω)\right)^{-1/2} \left(P_1(\mathrm{j}\,ω) - \right. \\
\left. - P_2(\mathrm{j}\,ω)\right) \left(I + P_1^*(\mathrm{j}\,ω)\ P_1(\mathrm{j}\,ω)\right)^{-1/2} \|_\infty
\end{aligned}
\tag{24}
$$

Figure 7 shows the frequency-dependent $ν$-gap metric of the 33 state low order and of the 97 state full order LPV models at all grid points. The $ν$-gap values are around 0.2 for up to 90 rad/s frequency and grow rapidly beyond the frequency range of interest. Therefore, the accuracy of the low order LPV model is good within the frequency range of interest.
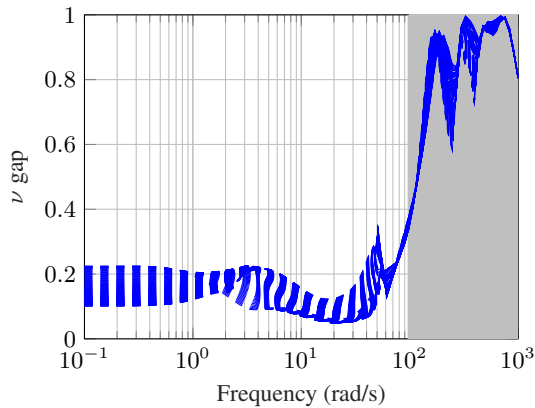

**Figure 7**: Variation of the $ν$-gap values for the 33 and 97 states LPV models

Bode diagram comparison—Figure 11 depicts Bode plots of the low and full order LPV models at 19 m/s and 24 m/s airspeeds. The low order model captures the input-output behavior of the full order model very well in the frequency range of interest.

Comparison with the Full Order Nonlinear Model

Time domain simulation is conducted to compare the low order LPV model with the full order nonlinear ASE model. The two models are run in open loop. The 33 state LPV model and the trim inputs of the 97 state nonlinear model are scheduled by $V_{s_{LPV}}$ and $V_{s_{NL}}$ respectively. The simulation starts with straight and level flight trim condition at $V_s = 18\,m/s$. The airspeed is then increased to approximately 24.5 m/s, slightly above the flutter speed, by adding a ramp signal to the throttle trim value. The models are excited by applying 5° doublets on the elevator and the aileron as shown in Figure 8. The responses of the low order LPV model and the full order nonlinear models are given in Figures 9 and 10. The two models show very similar behavior.
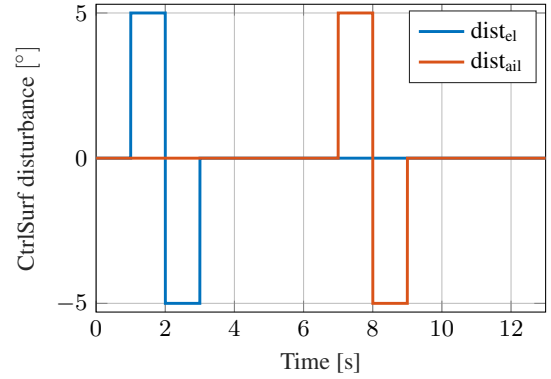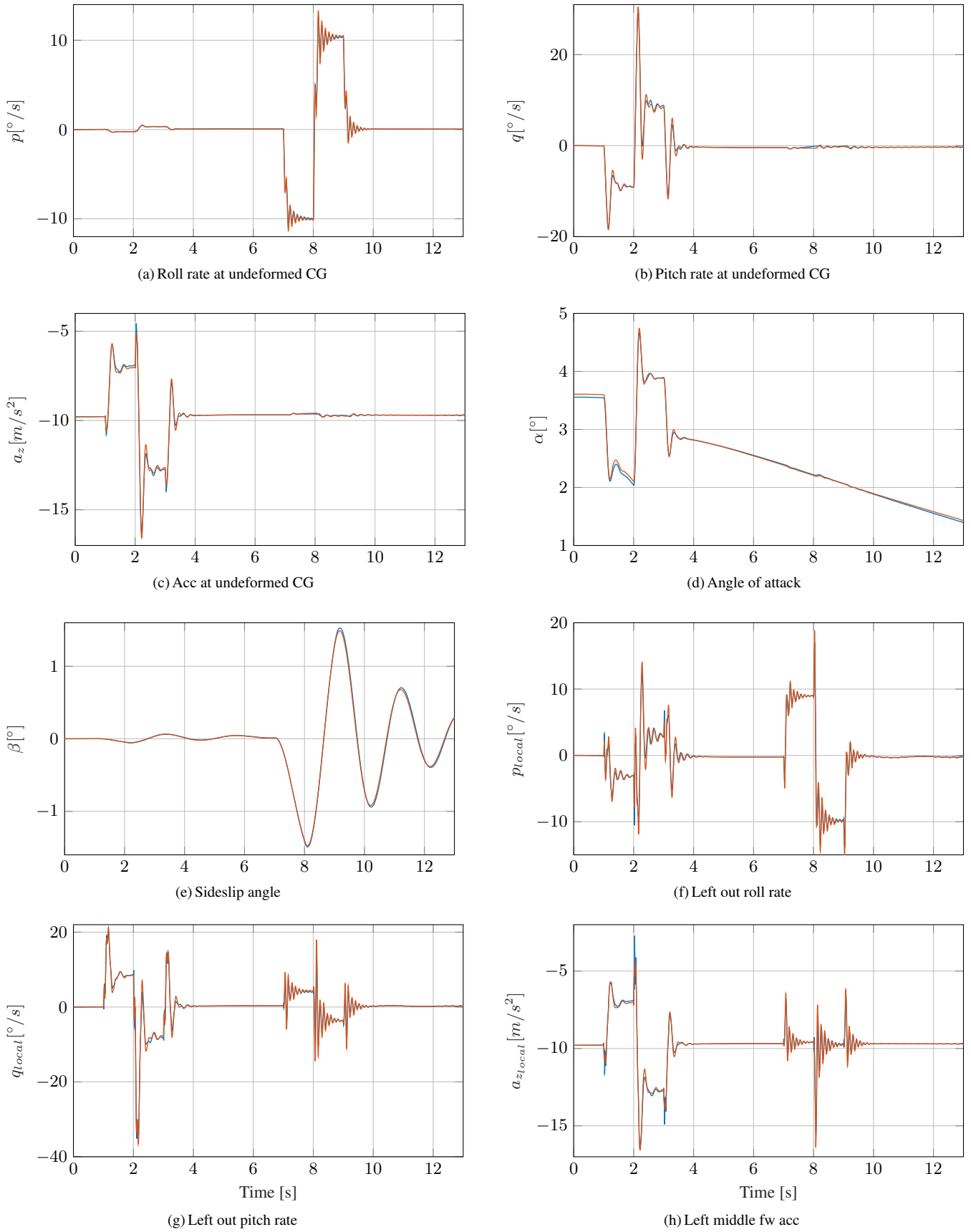

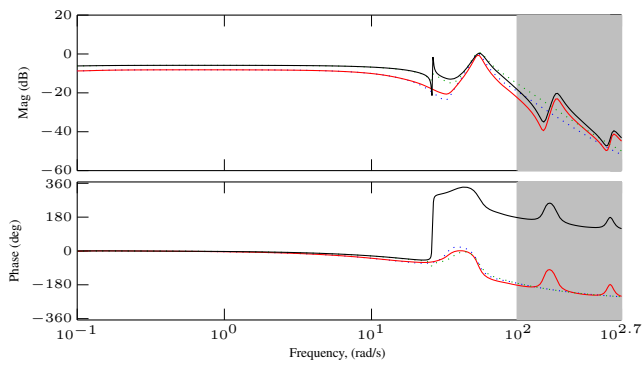**Figure 8**: Doublets acting as disturbance on the elevator and aileron
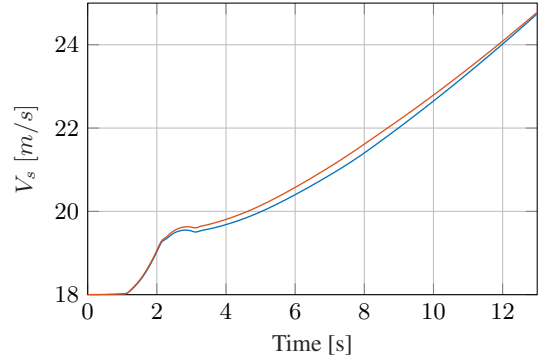
Figure 9: V_s of the nonlinear (——) and the LPV model (——)
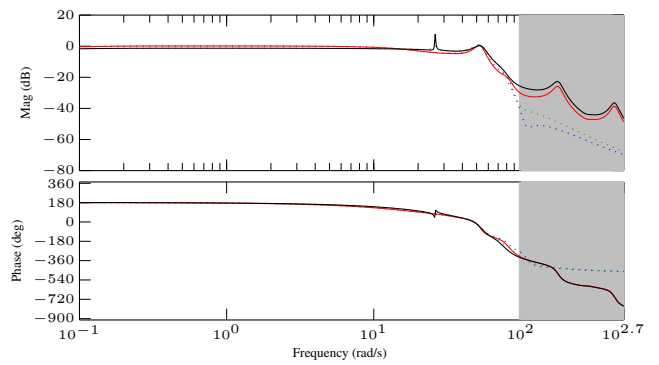
Future Steps

The future steps include developing a flutter suppression controller based on the low order ASE model and validating it on the full order model. In addition, the goal is to apply the proposed method for developing low order ASE models of the FLEXOP aircraft [40], which has more complex structural and aerodynamics components.
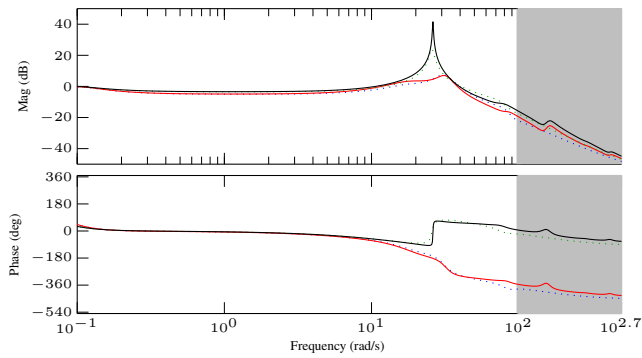
(a) Roll rate at undeformed CG

(b) Pitch rate at undeformed CG
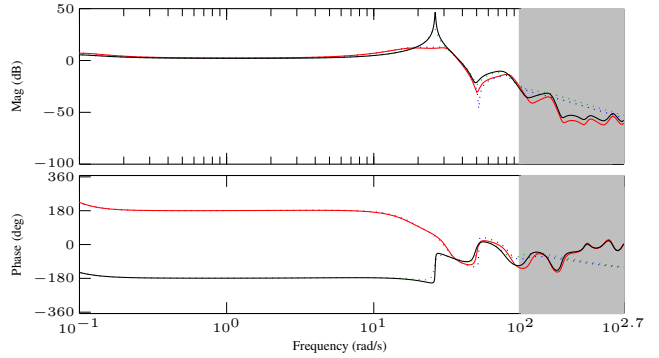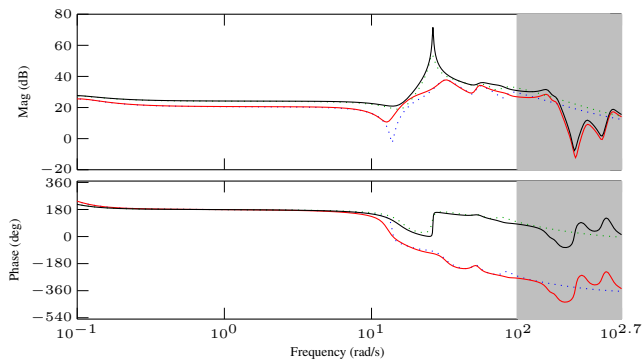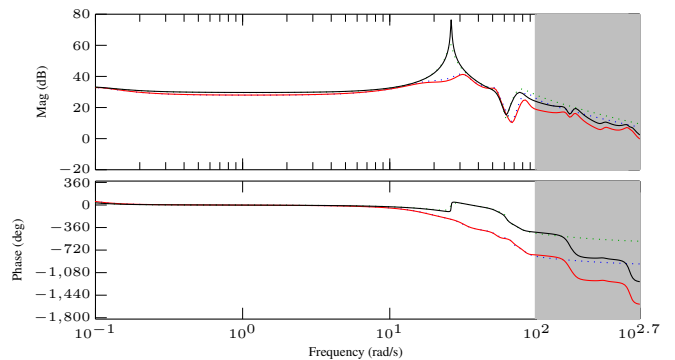
(c) Acc at undeformed CG

(d) Angle of attack

(e) Sideslip angle

(f) Left out roll rate

(g) Left out pitch rate

(h) Left middle fw acc

Figure 10: Responses of the nonlinear (——) and the LPV model (——)
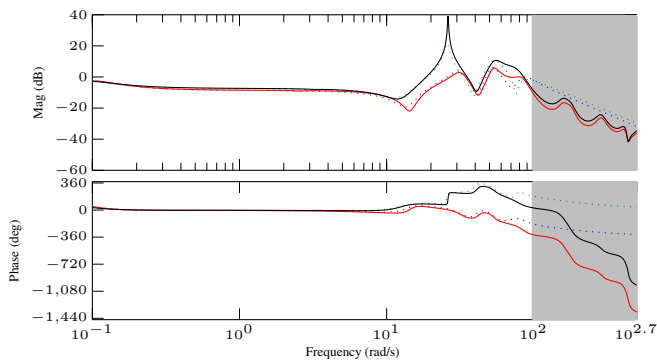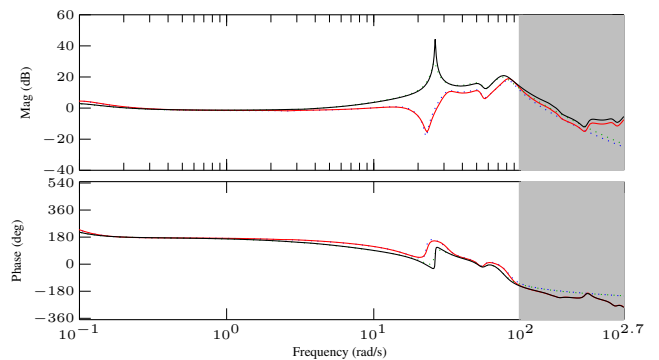
Figure 11: Bode plots of low order model at 19 m/s (⋯⋯) and 24 m/s (⋯⋯) and full order model at 19 m/s (——) and 24 m/s (——). The shaded gray area denotes the frequency range beyond the desired bandwidth of 100 rad/s

5. Conclusions

A "bottom-up" modeling approach is proposed for developing ASE aircraft models. The modeling is based on the subsystem ASE modeling, where the aerodynamics, structural dynamics and rigid body dynamics models are developed separately and then combined to from the ASE model. In general, these subsystems have simpler structure than the combined model. The key idea of the "bottom-up" modeling is therefore to reduce these components before combining them into the nonlinear ASE model. This way the proposed modeling approach avoids the application of challenging model order reduction techniques for LPV systems. In addition, the proposed modeling method preserves the physical meaning of the states. The approach is applied to develop a low order ASE model of the mini MUTT aircraft. The resulting nonlinear model is of 33 states upon which a grid based LPV model is obtained by Jacobian linearization. In order to assess the accuracy of the developed low order model a full order model is developed without reducing the subsystems. The ν-gap metric between the full order and the proposed low order model is around 0.2 everywhere in the frequency range of interest and all unstable modes of the mini MUTT aircraft are captured accurately. The Bode plots of the low and full order models show similar input-output behavior. In addition, time domain simulations show that the low order LPV model and the full order nonlinear models respond similarly to excitations that mimic wind gusts. Therefore, and with its much lower dynamic order, the low order model is expected to be well suited for control design. The next necessary step is to design a controller based on the low order model and validate it on the full order model.

Acknowledgments

References

[1] Y. Fung, *An introduction to the theory of aeroelasticity*, 1969.

[2] J. Theis, H. Pfifer, and P. Seiler, "Robust control design for active flutter suppression," in *AIAA Science and Technology Forum and Exposition*, 2016, pp. Paper No. AIAA–2016–1751.

[3] K. L. Roger, G. E. Hodges, and L. Felt, "Active flutter suppression-a flight test demonstration," *Journal of Aircraft*, vol. 12, no. 6, pp. 551–556, jun 1975.

[4] M. R. Waszak and S. Srinathkumar, "Flutter suppression for the active flexible wing - a classical design," *Journal of Aircraft*, vol. 32, no. 1, pp. 61–67, jan 1995.

[5] D. K. Schmidt, "Stability augmentation and active flutter suppression of a flexible flying-wing drone," *Journal of Guidance, Control, and Dynamics*, vol. 39, no. 3, pp. 409–422, mar 2016.

[6] A. Hjartarson, P. J. Seiler, A. Packard, and G. J. Balas, "LPV aeroservoelastic control using the LPVTools toolbox," in *AIAA Atmospheric Flight Mechanics (AFM) Conference*. American Institute of Aeronautics and Astronautics, aug 2013.

[7] J. S. Shamma, "Analysis and design of gain scheduled control systems," Ph.D. dissertation, Massachusetts Institute of Technology, Cambridge, 1988.

[8] G. Becker, "Quadratic stability and performance of linear parameter dependent systems," Ph.D. dissertation, University of California, Berkeley, 1993.

[9] F. Wu, "Control of linear parameter varying systems,"

Ph.D. dissertation, Univ. California, Berkeley, 1995.

[10] B. Takarics and P. Seiler, "Gain scheduling for nonlinear systems via integral quadratic constraints," in *American Control Conference*, 2015, pp. 811–816.

[11] C. Moreno, A. Gupta, H. Pfifer, B. Taylor, and G. Balas, "Structural model identification of a small flexible aircraft," in *American Control Conference*, 2014, pp. 4379–4384.

[12] A. Gupta, C. P. Moreno, H. Pfifer, B. Taylor, and G. J. Balas, "Updating a finite element based structural model of a small flexible aircraft." American Institute of Aeronautics and Astronautics, Jan. 2015.

[13] A. Kotikalpudi, "Robust flutter analysis for aeroservoelastic systems," Ph.D. dissertation, University of Minnesota, Twin Cities, 2017.

[14] D. K. Schmidt, W. Zhao, and R. K. Kapania, "Flight-dynamics and flutter modeling and analysis of a flexible flying-wing drone," in *AIAA Atmospheric Flight Mechanics Conference, AIAA SciTech Forum*, 2016.

[15] A. Kotikalpudi, C. Moreno, B. Taylor, H. Pfifer, and G. Balas, "Low cost development of a nonlinear simulation for a flexible uninhabited air vehicle," in *American Control Conference*, 2014, pp. 2029–2034.

[16] E. Albano and W. P. Rodden, "A Doublet-Lattice Method for Calculating Lift Distributions on Oscillating Surfaces in Subsonic Flows," *AIAA Journal*, vol. 7, no. 2, 1969.

[17] R. D. Milne, "Dynamics of the deformable aeroplane," *Aeronautical Research Council Reports and Memoranda*, no. 3345, 1964.

[18] S. Keyes, P. Seiler, and D. Schmidt, "A newtonian development of the mean-axis equations of motion for flexible aircraft," in *AIAA Science and Technology Forum and Exposition*, 2017, pp. Paper No. AIAA–2017–1395.

[19] D. K. Schmidt, *Modern Flight Dynamics*. McGraw-Hill, 2012, iSBN 9780073398112.

[20] L. Meirovitch and I. Tuzcu, "The lure of the mean axes," *Journal of Applied Mechanics*, vol. 74, no. 3, p. 497, 2007.

[21] D. K. Schmidt, "Discussion: "the lure of the mean axes" (meirovitch, l., and tuzcu, i., ASME j. appl. mech., 74(3), pp. 497–504)," *Journal of Applied Mechanics*, vol. 82, no. 12, p. 125501, oct 2015.

[22] S. A. Keyes, "A newtonian development of the mean-axis dynamics with example and simulation," Master's thesis, University of Minnesota, Twin Cities, 2017.

[23] G. D. Wood, "Control of parameter-dependent mechanical systems," Ph.D. dissertation, Univ. Cambridge, Cambridge, 1995.

[24] J. Theis, B. Takarics, H. Pfifer, G. Balas, and H. Werner, "Modal matching for lpv model reduction of aeroservoelastic vehicles," in *AIAA Science and Technology Forum*, 2015.

[25] C. Moreno, P. Seiler, and G. Balas, "Model reduction for aeroservoelastic systems," *Journal of Aircraft*, vol. 51, no. 1, pp. 280–290, 2014.

[26] J. Theis, P. Seiler, and H. Werner, "Lpv model order reduction by parameter-varying oblique projection," *IEEE Transactions on Control Systems Technology*, 2017.

[27] C. Poussot-Vassal and C. Roos, "Generation of a

reduced-order LPV/LFT model from a set of large-scale MIMO LTI flexible aircraft models," *Control Engineering Practice*, vol. 20, no. 9, pp. 919–930, sep 2012.

[28] I. Gozse, T. Luspay, T. Peni, Z. Szabo, and B. Vanek, "Model order reduction of LPV systems based on parameter varying modal decomposition," in *2016 IEEE 55th Conference on Decision and Control (CDC)*. IEEE, dec 2016.

[29] G. Liptak, T. Luspay, T. Peni, B. Takarics, and B. Vanek, "LPV model reduction methods for aeroelastic structures," in *20th IFAC World Congress*, 2017.

[30] C. D. Regan and B. R. Taylor, "mAEWing1: Design, build, test - invited," in *AIAA Atmospheric Flight Mechanics Conference*. American Institute of Aeronautics and Astronautics, jan 2016.

[31] A. Kotikalpudi, H. Pfifer, and G. Balas, "Unsteady aerodynamics analysis for a flexible unmanned aerial vehicle," in *AIAA Atmospheric Flight Mechanics Conference*, 2015.

[32] E. Burnett, C. Atkinson, J. Beranek, B. Sibbitt, B. Holm-Hansen, and L. Nicolai, "NDOF Simulation Model for Flight Control Development with Flight Test Correlation." American Institute of Aeronautics and Astronautics, Aug. 2010.

[33] J. Theis, H. Pfifer, and P. Seiler, "Robust control in flight: Active flutter suppression," in *AIAA Science and Technology Forum*, 2016.

[34] M. R. Waszak and D. K. Schmidt, "Flight dynamics of aeroelastic vehicles," *Journal of Aircraft*, vol. 25, no. 6, pp. 563–571, 1988.

[35] C. S. Buttrill, T. A. Zeiler, and P. D. Arbuckle, "Nonlinear simulation fo a flexible aircraft in maneuvering flight," in *Flight Simulation Technologies Conference, Guidance, Navigation, and Control and Co-located Conferences*, 1987.

[36] J. Katz and A. Plotkin, *Low-Speed Aerodynamics: From Wing Theory to Panel Methods (Mcgraw-Hill Series in Aeronautical and Aerospace Engineering)*. Mcgraw-Hill College, 1991.

[37] T. Kier and G. Looye, "Unifying manoeuvre and gust loads analysis models," in *International Forum on Aeroelasticity and Structural Dynamics*. American Institute of Aeronautics and Astronautics, 2009.

[38] R. K. L., "Airplane math modeling methods for active control design," in *Advisory Group for Aerospace Research and Development CP-228*, 1977.

[39] G. Vinnicombe, "Measuring robustness of feedback systems," Ph.D. dissertation, Univ. Cambridge, Cambridge, 1993.

[40] FLEXOP, "Flutter Free FLight Envelope eXpansion for ecOnomical Performance improvement (FLEXOP)," Project of the European Union, Project ID: 636307, 2015-2018.

BIOGRAPHY

Béla Takarics *received his M.S. and Ph.D. degree in mechanical engineering from the Budapest University of Technology and Economics, Budapest, Hungary, in 2007 and 2012, respectively. He is currently a research fellow at the Systems and Control Lab (SCL) of the Research Institute for Computer Science and Control of the Hungarian Academy of Sciences (MTA SZTAKI). His research interests include linear parameter varying systems, IQC based robust control and aeroservoelastic systems.*

Bálint Vanek *received his MSc degree in mechanical engineering from the Budapest University of Technology and Economics, Budapest, Hungary, in 2003 and a Ph.D. in aerospace engineering from the University of Minnesota, Department of Aerospace Engineering and Mechanics in 2008. He is currently a senior research fellow and leader of the Aerospace Guidance, Navigation, and Control Group at the Systems and Control Lab (SCL) of the Research Institute for Computer Science and Control of the Hungarian Academy of Sciences (MTA SZTAKI). His research interests include flight control, fault detection, unmanned aerial vehicles (UAVs), inertial and satellite navigation systems.*
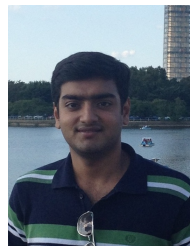
Aditya Kotikalpudi *received his MSc degree in aerospace engineering from the Indian Institute of Technology, Kharagpur, India in 2012 and a Ph.D. in aerospace engineering from the University of Minnesota, Department of Aerospace Engineering and Mechanics in 2016. He is currently a research engineer at Systems Technology Inc. His research interest include flutter analysis and aerodynamics modeling for flexible aircraft.*

Peter Seiler *received his Ph.D. from the University of California, Berkeley in 2001. His graduate research focused on coordinated control of unmanned aerial vehicles and control over wireless networks. From 2004 2008, he worked at the Honeywell Research Labs on various aerospace and automotive applications including the redundancy management system for the Boeing 787, sensor fusion algorithms for automotive active safety systems and re-entry flight control laws for NASAs Orion vehicle. Since joining the University of Minnesota in 2008, he has been working on fault-detection methods for safety-critical systems and advanced control techniques for wind turbines and unmanned aircraft.*